Monthly Notices
of the
ROYAL ASTRONOMICAL SOCIETY

Mon. Not. R. Astron. Soc. **425,** 1696–1708 (2012) doi:10.1111/j.1365-2966.2012.21607.x

Modelling the composition of a young star cluster ejecta

Mercedes Mollá[1]★ and Roberto Terlevich[2,3]†

[1]*Departamento de Investigación Básica, CIEMAT, Avda. Complutense 40, E-28040 Madrid, Spain*
[2]*INAOE, Luis Enrique Erro 1, Tonanzintla, Puebla 72840, Mexico*
[3]*Institute of Astronomy, University of Cambridge, Madingley Road, Cambridge CB3 0HA*

Accepted 2012 June 27. Received 2012 June 27; in original form 2011 September 23

ABSTRACT

We have computed with a fine time grid the evolution of the elemental abundances of He, C, N and O ejected by young ($t < 20$ Myr) and massive ($M = 10^6$ M$_\odot$) coeval stellar cluster with a Salpeter initial mass function (IMF) over a wide range of initial abundances. Our computations incorporate the mass loss from massive stars ($M \geq 30$ M$_\odot$) during their wind phase including the Wolf–Rayet phase and the ejecta from the core-collapse supernovae. We find that during the Wolf–Rayet phase ($t < 5$ Myr) the cluster ejecta composition suddenly becomes vastly overabundant in N for all initial abundances and in He, C and O for initial abundances higher than one-fifth of the solar. The C and O abundances in the cluster ejecta can reach over 50 times the solar value with important consequences for the chemical and hydrodynamical evolution of the surrounding interstellar medium.

Key words: stars: abundances – stars: mass-loss – supernovae: general – stars: Wolf–Rayet – galaxies: abundances – galaxies: star clusters: general.

1 INTRODUCTION

Massive young stellar clusters are ideal laboratories for research into the evolution of massive stars and their interaction with their surrounding interstellar medium (ISM). These luminous and rapidly evolving massive stars supply most of the young cluster ultraviolet radiation that creates the encompassing H II region and a large amount of mass and mechanical energy in the forms of supernova ejecta and stellar winds particularly during the Wolf–Rayet (WR) phase. These massive star-forming regions can eject during their first 10 Myr of evolution about 20 per cent of their initial mass Leitherer et al. (1999, hereinafter STB99) mostly in the form of newly synthesized C, N and O that by mass represent most of the heavy elements.

Massive young stellar clusters are ubiquitous particularly among late-type galaxies. Their stellar wind phase can result in a supergalactic wind affecting the nearby intergalactic medium (IGM). It is open to question how the ejected freshly synthesized heavy elements cools and mix with the ISM, and how long this process governed by the cooling time-scale may last. The time-scale for cooling is strongly dependent on the gas cooling rate that in turn is dependent on the gas chemical composition and density (e.g. Tenorio-Tagle 1996; Kobulnicky et al. 1997; Kobulnicky & Skillman 1998; van Zee & Haynes 2006; López-Sánchez & Esteban 2010). Thus evaluating the composition of the cluster ejecta and its time evolution is a necessary prior step for estimates of the evolution of the cooling function and the computation of cooling and feedback time-scales. Although work like that of Silich et al. (2001) underlined the large influence that the enrichment of the stellar ejecta can have on the radiative cooling of starburst superbubbles, many researchers are still using Raymond, Cox & Smith (1976) radiative cooling coefficient calculation for solar abundances when modelling the interaction between the stellar ejecta and their surrounding medium.

In this paper we present a set of models designed to calculate in detail the first 20 Myr of the evolution and chemical composition of a star cluster ejecta on very short time-scales, i.e. much shorter than the H II region lifetime, and in particular to resolve the WR wind phase

Galactic chemical evolution models traditionally assume that the elements ejected by the stellar cluster are incorporated to the ISM when the corresponding stars die, i.e. at a time equal to their lifetimes (Portinari, Chiosi & Bressan 1998; Dray & Tout 2003; Dray et al. 2003). The shortest time step is usually defined by the mean lifetime of the most massive star. Since this is typically around 100–120 M$_\odot$, chemical evolution calculations begin normally at around 3–5 Myr with comparable time steps. This way, important phases of the wind evolution, occurring before 3 Myr or short lived like the WR phase, are lost or diluted.

To compute the composition of the ejecta, most chemical evolution models use the total yields of elements due to supernova explosions, such as those given by Woosley & Weaver (1995, WW95) or other more recent works (Rauscher et al. 2002; Umeda & Nomoto 2002; Limongi & Chieffi 2003; Chieffi & Limongi 2004; Fröhlich et al. 2006; Heger & Woosley 2010) to calculate the total change of the elemental abundances. Other computations include the elements ejected during the wind phase of massive stars (Maeder

★E-mail: mercedes.molla@ciemat.es
†Visiting Professor at UAM, Madrid.

1992; Meynet & Maeder 2002; Hirschi, Meynet & Maeder 2005; Kobayashi et al. 2006; Hirschi 2007), only the models of Portinari et al. (1998, hereinafter PCB98) include the evolution of both phases, i.e. the yields of core-collapse supernova explosions from Woosley & Weaver (1995) and the stellar wind yields produced during the evolution of each star. However, PCB98 computations, as most chemical evolution models, were performed with time steps much longer than the lifetime of an H II region therefore missing short-lived stages like the WR phase. Moreover, the evolution of a supernova progenitor that loses part or most of its mass is not the same as a normal main sequence massive star. Since mass and structure are substantially different in he time of the supernova explosion, the associated yields will also differ, such as it is explained in Woosley, Langer & Weaver (1993, 1995, hereinafter WLW93, WLW95, respectively). To take this into account, PCB98 linked the final stage of the star after lost mass with the supernova yields though the CO core mass. However, they use the WW95 yields instead WLW93/WLW95 yields.

The organization of this paper is as follows. In Section 2 we use O and WR winds computations to estimate the evolution of the ejecta of a young massive stellar cluster. In Section 3 we compute the contribution of the explosive nucleosynthesis. Section 4 gives the complete evolution of elemental abundances within the cluster and discusses the impact of each contribution over the final ejecta. Our conclusions are given in Section 5.

2 STELLAR WIND COMPOSITION

To compute the evolution of the rate of ejection of elements due to stellar winds of a single stellar population (SSP) of a given initial metallicity and initial mass function (IMF), we have used the tables resulting from the isochrones calculation by Bressan, Bertelli & Chiosi (1993) and Fagotto et al. (1994a,b). These authors give the amount of mass lost by massive stars during their evolution for seven initial stellar masses: 12, 15, 20, 30, 40, 60 and 100 $M_\odot$. For each initial mass and time step, the tables provide the present mass (in solar mass units), the rate of mass loss in $M_\odot\ yr^{-1}$ (logarithmic scale) and the abundances of the stellar surface for H, ^{4}He, ^{12}C, ^{14}N and ^{16}O. These tables are provided for six initial metallicities: $Z =$ 0.0001, 0.0004, 0.004, 0.008, 0.02 and 0.05.

In Fig. 1 we plot the evolution of the mass-loss rate for all stellar masses. The mass-loss rate depends strongly on the initial stellar mass and composition. It is clear from the figure that the lowest mass stars maintain for a long time a low mass-loss rate, while the most massive ones evolve rapidly ejecting a large part of their mass in discrete events. An important consequence is that a star of solar metallicity with an initial mass of 100 $M_\odot$ ends its life with around 7 $M_\odot$, while the evolution of star of 12 $M_\odot$ may be followed for almost 20 Myr at a very low mass-loss rate that implies that its total mass remains roughly constant.

The mass-loss rate is also dependent on the metallicity through the semi-empirical relation included in the stellar models (see Bressan et al. 1993, for details). We see these differences in Fig. 1 where the evolution for the six given metallicities stars is shown. The lower the metallicity, the smaller the mass-loss rate and smoother the behaviour shown on the mass-loss rate evolution.

In Table 1 we summarize some characteristics of the stellar input models: for each metallicity Z, column 1, and initial stellar mass m_*, column 2, the final mass $m_{\rm end}$ is listed in column 3, and the final evolutionary time $t_{\rm end}$ in Myr is in column 4. Column 5 shows the final surface abundance (in mass fraction) of H, $X_{\rm f,H}$ (which we will use to determine the mass of the helium core in Section 3).

Since each stellar mass table has a different time range and time step, we have performed a linear interpolation to obtain values at the same times for all masses. The normalized table is provided in as Supporting Information with the online version of the article for all calculated metallicities and masses. Table 2 shows, as an example, a few time steps of the most massive star of $Z = 0.02$. It gives for the metallicity of column 1 and for the seven stellar masses, defined by column 2, the initial mass m_* in solar mass units in column 3, the time in Myr units in column 4, the mass-loss rate, $\dot{m}$, in units of solar mass per year, in column 5, the elemental abundances of H, ^{4}He, ^{12}C, ^{14}N, and ^{16}O[1] as fractions in mass, in columns 6–10, and the stellar mass $m(t)$ at a given time t in column 11.

The evolution of the stellar masses and surface abundances is shown with dots in Fig. 2. Each type and colour of line indicate a stellar mass as labelled. The lines show the results of the numerical interpolation used in the following sections. In panel (a) we see how drastically the stellar mass decreases when $m > 30\,M_\odot$ in times as short as 5 Myr. The evolution of the stellar surface abundances for H, He in total mass fraction and C, N, and O, as abundances in mass, X, is shown in panels (b) to (f) of the same Fig. 2. The surface abundances of C, N and O show a large increase following the start of the stellar winds revealing the product of first hydrogen and then helium burning. This fact combined with a depletion of H in the ejecta means that if these abundances were represented as abundances in number, $12 + \log(X/H)$, they would be very high.

To compute the evolution of a stellar cluster ejecta we have assumed that the cluster stellar mix consists of a coeval population or SSP where all stars were created simultaneously and with the same metallicity. By using the normalized tables of the previous paragraph, it is easy to calculate in each time step the contribution of each star, m, weighted by the number of stars in its mass range, given by the IMF $\Phi(m)$. Thus, for each element i and each time t

$$m_{{\rm ej},i}(t) = \int_{m_{\rm low}}^{m_{\rm up}} \int_{\Delta t} {\rm e}_{z,i}(m, t')\phi(m)\ {\rm d}m\ {\rm d}t', \qquad (1)$$

where

$${\rm e}_{z,i}(m, t') = XS_i(m, t')\dot{m}(t'). \qquad (2)$$

$XS_i(m, t)$ is the surface abundance of each element i and $\dot{m}(t)$ is the mass-loss rate for each stellar mass m in every time t.

We have performed the calculations for six different IMFs: (1) a Salpeter (1955) law, $\Phi(m) \propto m^{-x}$, with an exponent $x = -2.35$ (hereinafter SAL), and five others from (2) Miller & Scalo (1979, hereinafter MIL), (3) Ferrini, Penco & Palla (1990, hereinafter FER), (4) Kroupa (2001, hereinafter KRO), (5) Chabrier (2003, hereinafter CHA), all of them with limits $m_{\rm low} = 0.15$ and $m_{\rm max} = 100\,M_\odot$, and (6) a Salpeter law with limits $m_{\rm low} = 1.00$ and $m_{\rm max} = 100\,M_\odot$ as the one used in STB99. Our tables are therefore calculated for all these IMFs, but in the next figures only Salpeter results are shown since it is a widely used IMF.

The integration is done for the whole mass range of the IMF in each time step. To integrate in time we have chosen a time step $\delta t = 0.01$ Myr (small enough to follow the rapid evolution of the mass-loss process without losing any phase). To integrate in mass it is necessary to be available a grid with a wide range of masses. So, we have performed a careful interpolation in mass using the seven existing tables. The method to obtain the mass-loss rate for any mass value is not straightforward, since it shows abrupt changes in

[1] For the sake of simplicity we write He, C, N and O for ^{4}He, ^{12}C, ^{14}N and ^{16}O along the text.

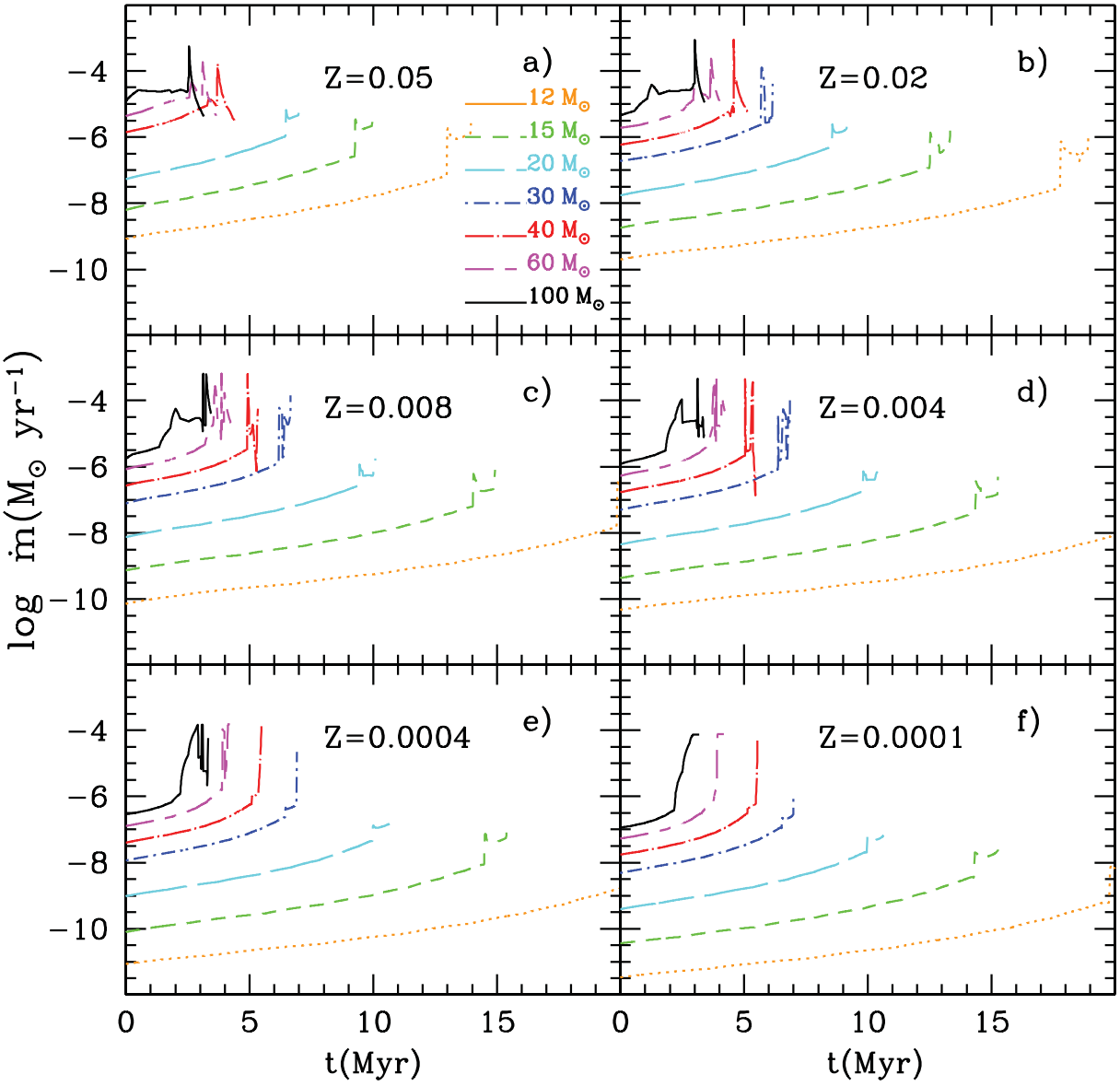

Figure 1. Evolution of the mass-loss rate for the stars given by the Padova group for different metallicities Z as labelled. Colour and type of lines mean a different value of stellar mass as labelled.

small time-scales. So we have used the tables of the mass-loss rate to calculate the actual mass $m(t)$ in any time with high accuracy. Then we have interpolated between these values for obtaining a new curve for each mass m, and finally we compute the mass-loss rate from this $m(t)$. To calculate the elemental abundances, we have taken into account the different phases of each element abundance, interpolating between two known masses to obtain the points limiting these phases for each mass m. All computations were done for a SSP cluster with a total mass in stars of 10^6 M$_\odot$.[2]

In Fig. 3 we show the resulting evolution of the instantaneous ejecta abundances X for He, C, N and O in mass as before. Initial abundances are the ones included in the original files for $Z = 0.0001$, 0.0004, 0.004, 0.008, 0.02 and 0.05. If we take the solar abundances from Asplund et al. (2009) as reference, which implies a total $Z_\odot = 0.0142$, the $Z = 0.02$ abundances, indicated in the figure as dotted grey lines, are in fact ∼0.15 dex higher than the adopted solar values. If we analyse the results for $Z = 0.02$ (red lines), we see that cluster ejecta abundances are not always equal to the initial value. It is evident that ejecta abundances show strong variations in the WR stars phase, which may reach up to two orders of magnitude over the initial value for each metallicity. Thus, He and N increase in a first phase, when C and O decrease. Then N and He decrease again just when C and O increase.

This effect is strongly dependent on the original metallicity of the stellar cluster as we may see by comparing with the other metallicity lines. The initial values for the non-solar cases are indicated with arrows around the values, +0.3, −0.4, −0.7, −1.7 and −2.3 dex. For the two models with the lowest metallicity, the ejecta abundances, in particular C and O, do not differ very much from the initial values

[2] It is necessary to take into account that we will give averaged values for this stellar cluster mass. For stellar clusters less massive than 10^4 M$_\odot$, the stochastic effects over the IMF are important (Cerviño & Luridiana 2004, 2006) and they may change the stellar mass distribution and the corresponding results compared with those we obtain.

Table 1. Characteristics of the stellar models.

Z	m_* ($M_\odot$)	m_{end} ($M_\odot$)	t_{end} (Myr)	$X_{f,H}$
0.0001	12	11.99	21.17	0.748
0.0001	15	14.98	15.28	0.731
0.0001	20	19.93	10.65	0.701
0.0001	30	29.69	7.00	0.770
0.0001	40	38.93	5.52	0.770
0.0001	60	37.31	4.19	0.681
0.0001	100	67.39	3.18	0.649
0.0004	12	11.97	21.39	0.741
0.0004	15	14.94	15.39	0.727
0.0004	20	19.83	10.64	0.699
0.0004	30	29.35	6.91	0.673
0.0004	40	35.66	5.46	0.693
0.0004	60	31.89	4.20	0.486
0.0004	100	55.45	3.32	0.142
0.004	12	11.84	21.47	0.716
0.004	15	14.76	15.26	0.705
0.004	20	19.30	10.48	0.686
0.004	30	19.05	6.86	0.544
0.004	40	16.86	5.44	0.241
0.004	60	17.55	4.20	0.000
0.004	100	46.93	3.38	0.080
0.008	12	11.77	21.07	0.708
0.008	15	14.62	14.92	0.693
0.008	20	19.03	10.10	0.671
0.008	30	13.05	6.66	0.516
0.008	40	16.44	5.31	0.000
0.008	60	10.87	4.22	0.000
0.008	100	14.23	3.44	0.000
0.02	12	11.50	18.93	0.667
0.02	15	14.21	13.34	0.655
0.02	20	18.06	9.17	0.630
0.02	30	12.63	6.15	0.000
0.02	40	5.35	5.14	0.000
0.02	60	6.01	4.13	0.000
0.02	100	7.16	3.40	0.000
0.05	12	10.85	13.95	0.577
0.05	15	13.12	9.97	0.565
0.05	20	16.05	6.99	0.539
0.05	30	9.84	5.15	0.000
0.05	40	3.63	4.36	0.000
0.05	60	4.11	3.63	0.000
0.05	100	4.22	3.11	0.000

except for the decrease around 4–5 Myr. However, for higher initial metallicities, all lines show a strong sudden increase at around 4.5–5 Myr reaching values one or two orders of magnitude larger than the initial value and lasting few million years.

For N the behaviour is however different. For all models the N abundance in the ejecta increases at 3 Myr, even at the lowest metallicities. After about 5–8 Myr of evolution, when the cluster turn-off mass is below 25 $M_\odot$, the ejecta metallicity asymptotically approaches the initial value for all initial compositions, except again for N which maintains a higher value than the initial one. Probably this may be explained by the fact that the convective envelope dredges up the modified composition of CNO from the inner parts of the star up to the surface during the red supergiant (RSG) phase, which enhances the N mass fraction, slightly reducing C and O abundances.

The resulting accumulated ejected masses for the cluster in every time step are given in Table 3. For each IMF, column 1, and metallicity, given in column 2, we give the time step in Myr in column 3, the total ejected mass in column 4, and the accumulated ejected mass of the different elements in columns 5–9 for H, He, C, N and O. We show an example here for solar metallicity and a Salpeter IMF; the complete tables for all times, metallicities and IMFs will be provided as Supporting Information with the online version of the article.

The evolution of the accumulated ejecta abundances shows in Fig. 4(a) sharp increase for $Z \geq 0.008$ due to the mass loss of massive stars followed by a plateau after the peak of mass loss associated with the WR stars decline. For the models with the lowest metallicities, C and O abundances do not change much in relation with the initial values, as explained before, decreasing slightly, simultaneously to the increase of N. However, for the other metallicities the increase in C and O abundances is quite large. On the other hand, He and N abundances, even at the lowest metallicity cases, show the sharp increase at 3 Myr followed by a plateau that shows an enrichment with respect to the initial value larger than 0.5 dex in most cases. This increase in the He and N abundance may have important consequences for measurements of the chemical composition of galaxies based on abundances estimated using emission lines from H II regions particularly for the lowest metallicity regions, i.e. those with $12 + \log(O/H) \leq 7.3$.

These huge variations in the abundances of the ejecta of a stellar cluster may also be important for the hydrodynamical evolution of the ISM. The high metallicity might lead to extremely short cooling times in the ejecta with important consequences for the subsequent feedback.

3 ADDING THE SUPERNOVA EJECTA TO THE STELLAR WINDS

In this section we include the elements produced by supernova in our calculations. Stars more massive than $m \geq 12\,M_\odot$ end their evolution as core-collapse supernovae. New elements are

Table 2. Surface abundances of the stellar models for each mass for $Z = 0.02$. Similar complete tables for the six metallicities and seven stellar masses will be provided as Supporting Information with the online version of the article.

Z	N	m_* ($M_\odot$)	t (Myr)	$\dot{m}$ ($M_\odot\,yr^{-1}$)	X_H	X_{He}	X_C	X_N	X_O	$m(t)$ ($M_\odot$)
0.02	7	100.0	1.300	0.364E−04	0.687E+00	0.293E+00	0.434E−02	0.271E−02	0.963E−02	87.49
0.02	7	100.0	1.310	0.358E−04	0.684E+00	0.296E+00	0.418E−02	0.312E−02	0.937E−02	87.25
0.02	7	100.0	1.320	0.351E−04	0.680E+00	0.300E+00	0.402E−02	0.353E−02	0.911E−02	87.00
0.02	7	100.0	1.330	0.345E−04	0.676E+00	0.304E+00	0.386E−02	0.394E−02	0.885E−02	86.76
0.02	7	100.0	1.340	0.338E−04	0.672E+00	0.308E+00	0.370E−02	0.435E−02	0.859E−02	86.51
0.02	7	100.0	1.350	0.332E−04	0.668E+00	0.312E+00	0.354E−02	0.476E−02	0.832E−02	86.27
0.02	7	100.0	1.360	0.325E−04	0.664E+00	0.316E+00	0.338E−02	0.518E−02	0.806E−02	86.02

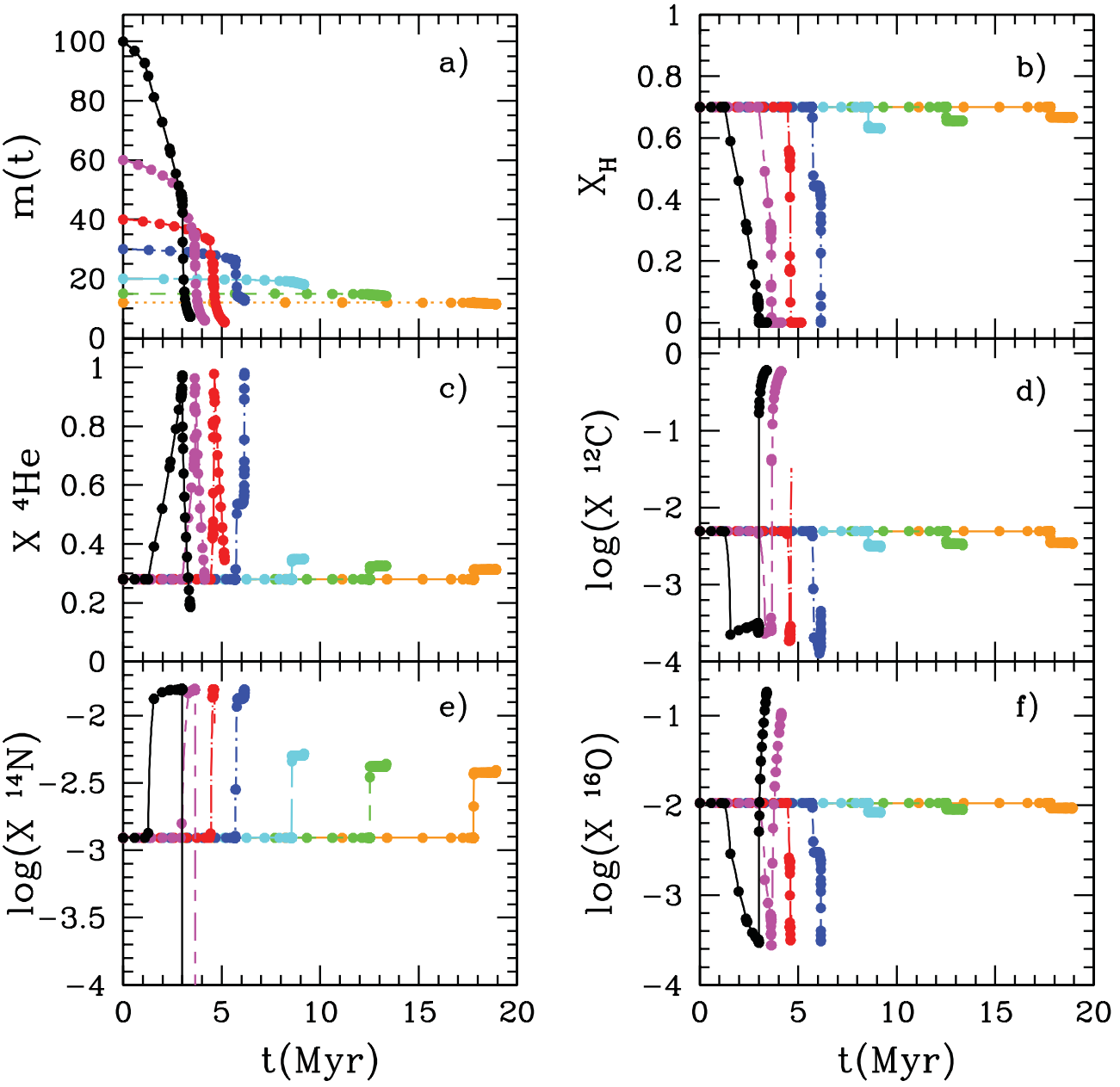

Figure 2. Input stellar parameters for $Z = 0.02$. The evolution of the stellar mass is shown in panel (a) and the evolution of the surface abundances is shown in panels (b) to (f) for the same initial stellar masses as labelled in Fig. 1. The dots represent the actual results from the stellar evolutionary models, while the lines are the interpolation in time used in this work.

created and ejected in these events. Since we assume an IMF where the most massive star $m_{\rm max} = 100\,{\rm M}_{\odot}$ has a mean lifetime of $\tau = 3.7$ Myr, the ejections are zero before this time. Only after 3.7 Myr supernovae begin to contribute to the cluster ejected mass.

In computing the total ejected mass and its composition, an important effect to take into account is that due to the stellar wind the mass of a star at the pre-supernova stage is smaller than its main-sequence mass. Thus, the supernova yields for a given star are not those corresponding its main-sequence mass since the star which explodes is less massive. To estimate the supernova yields we took as the supernova progenitor mass the mass of each star at the end of its wind phase. In practice, the models behave in two different ways depending on the wind mass-loss rate.

(i) *Small mass-loss rate*. Stars with initial masses around $15\,{\rm M}_{\odot}$ lose only part of their H, therefore $X_{\rm H} > 0$ at all times. For example, stars with $Z = 0.02$ and initial masses 12, 15 and $20\,{\rm M}_{\odot}$ end the winds phase with 11.46, 14.21 and $18.06\,{\rm M}_{\odot}$, respectively. In this case, and even more so for smaller abundances, it is reasonable to assign them the WW95 models in the same way as PCB98 did. In those cases we simply use the final mass of each star to select the most appropriate model among the models given by WW95.

(ii) *High mass-loss rate*. Stars with $Z \geq 0.008$ and $M \geq 30\,{\rm M}_{\odot}$ have high mass-loss rates and arrive to the end of the wind phase without H envelope inducing important changes to the supernova explosion mechanism and ejecta. For this case we adopted the models by WLW93 and WLW95, respectively. WLW95 calculated the

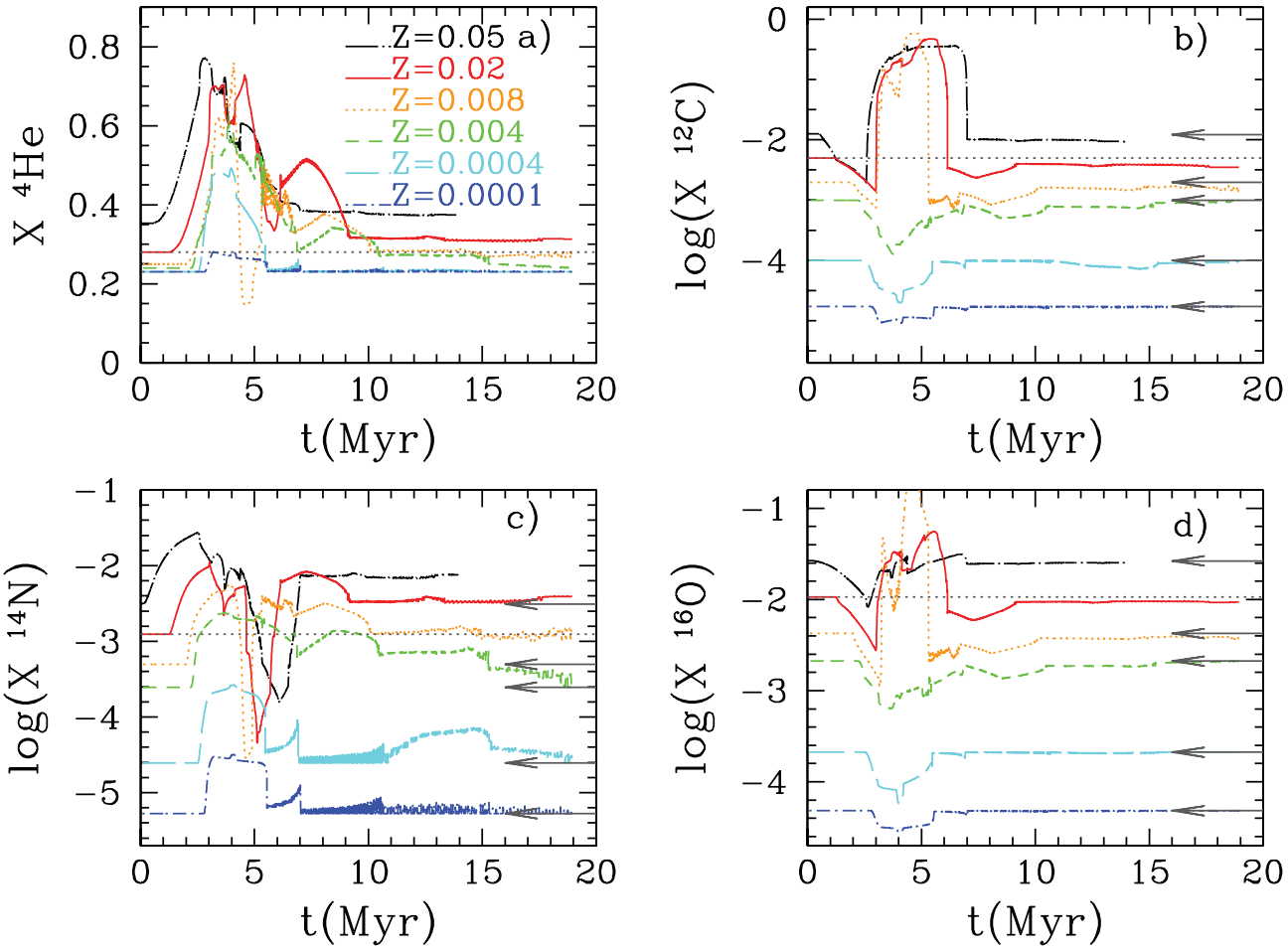

Figure 3. Evolution of the instantaneous abundances in mass for a stellar cluster due to stellar wind integrated for a Salpeter IMF: (a) He, (b) C, (c) N and (d) O for $Z = 0{,}05$, 0.02, 0.008, 0.004, 0.0004 and 0.0001 with different coded lines as labelled in panel (a). In each panel the dotted grey line marks the initial abundance for $Z = 0.02$ and the arrows mark the initial values for the other metallicities.

Table 3. Accumulated masses ejected by a stellar cluster of 10^6 $M_\odot$ during its wind phase for 20 Myr for $Z = 0.02$ and a Salpeter IMF. The complete tables for all times, metallicities and IMFs will be provided as Supporting Information with the online version of the article.

IMF	Z	Time (Myr)	m_{ej} ($M_\odot$)	H ($M_\odot$)	He ($M_\odot$)	C ($M_\odot$)	N ($M_\odot$)	O ($M_\odot$)
SAL	0.0200	0.50	0.753E+03	0.527E+03	0.210E+03	0.372E+01	0.934E+00	0.798E+01
SAL	0.0200	0.51	0.770E+03	0.539E+03	0.215E+03	0.380E+01	0.954E+00	0.816E+01
SAL	0.0200	0.52	0.787E+03	0.550E+03	0.220E+03	0.388E+01	0.975E+00	0.834E+01
SAL	0.0200	0.53	0.804E+03	0.562E+03	0.225E+03	0.397E+01	0.996E+00	0.852E+01
SAL	0.0200	0.54	0.821E+03	0.574E+03	0.229E+03	0.405E+01	0.101E+01	0.870E+01
SAL	0.0200	0.55	0.838E+03	0.586E+03	0.234E+03	0.414E+01	0.103E+01	0.888E+01
SAL	0.0200	0.56	0.855E+03	0.598E+03	0.239E+03	0.422E+01	0.106E+01	0.906E+01
SAL	0.0200	0.57	0.872E+03	0.610E+03	0.244E+03	0.430E+01	0.108E+01	0.924E+01

evolution of stars between 4 and 20 $M_\odot$ without H envelope. Their results are given for a range of masses of helium core m_{He}, defined as the mass at which the abundance of H falls to zero. After H exhaustion, these stars continue losing mass. A star of $m_{He} = 20\,M_\odot$ loses 16.44 $M_\odot$, ending with a mass of 3.55 $M_\odot$. Then, it explodes ejecting other 2.00 $M_\odot$ and keeping 1.55 $M_\odot$ in the remnant. In a similar way a star of $m_{He} = 7.00\,M_\odot$ loses 3.80 $M_\odot$ ending with 3.20 $M_\odot$ before exploding, ejecting 1.70 $M_\odot$ and producing a remnant of 1.50 $M_\odot$.

Using the Padova tracks we obtain, for the seven original values of stellar masses, the mass of each star when H is depleted from the envelope. These values are shown in Table 4 for $Z \geq 0.008$ given that for metallicities lower than this the condition $X_H = 0$ is never reached. The relation between the initial mass in the main sequence m_* and the mass of the He core m_{He} is shown in Fig. 5 where we see that the behaviour is quite smooth with the resulting m_{He} ranging from 10 to 45 $M_\odot$. The explosive yields for masses m_{He} between 4 and 20 $M_\odot$ are taken from WLW95. For masses higher than 20 $M_\odot$,

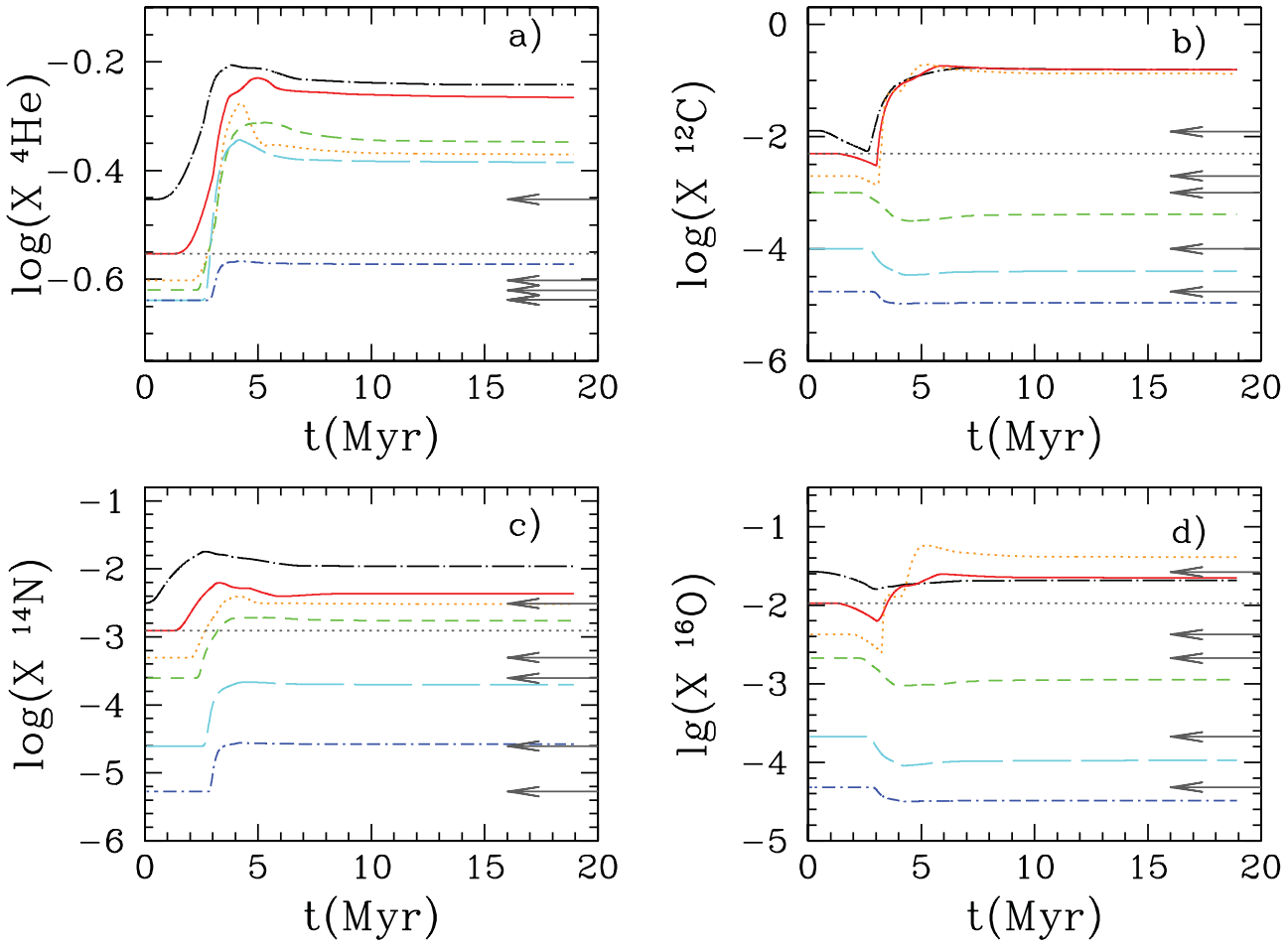

Figure 4. Evolution of abundances in mass of the accumulated masses ejected by a stellar cluster for (a) He, (b) C, (c) N and (d) O. The metallicities are shown with the same colour codes as in the previous figure. The dotted line and the arrows have the same meaning than in Fig. 3.

Table 4. Stellar mass–He core mass relation for Padova stellar tracks.

	Z		
	0.008	0.02	0.05
m_*		$M_{\rm He}$	
30	–	12.05	9.84
40	17.04	14.50	15.56
60	25.44	27.80	20.13
100	45.14	42.20	28.44

we take the results from WLW93 where the evolution of WR stars is computed starting at $X_{\rm H} = 0.50$. For models with initial mass of 60 and 85 $M_\odot$ (which begin the RSG or luminous blue variable (LBV) phase with 55.5 and 76.9 $M_\odot$, respectively), the resulting He core masses are $m_{\rm He} = 26.3$ and 45.3 $M_\odot$, respectively, their masses at the end of the wind phase being only 4.25 and 8.30 $M_\odot$. These models are very similar to our most massive stars of 60 and 100 $M_\odot$, for which $m(X_{\rm H} = 0.50)$ are 44.4 and 80 $M_\odot$, with $m_{\rm He} =$ 27.8 and 44.9 $M_\odot$ and with final masses of 5.93 and 7.16 $M_\odot$.

In Fig. 6 we show the comparison between the evolution of the most massive stars used here with the final results of WLW93/WLW95. Note that the final masses in the Padova models for $Z = 0.02$ are slightly larger than the ones from WLW95/WNL93 with the exception of the most massive model. For this case the Padova model reaches 7.17 $M_\odot$ at the end of the evolution, while the corresponding model from WLW93 has a slightly higher value (8.30 $M_\odot$).

Thus, to compute the explosive yields for massive stars with high mass-loss rate, we proceeded as follows: for each time step of our Table 3, we calculate the stellar mass that corresponds to the stellar mean lifetime $\tau(m) = t$. Interpolating in Table 4 we obtain $m_{\rm He}$, i.e. the mass of the star at $X_{\rm H} = 0$. We use this value of $m_{\rm He}$ to interpolate with the adequate value of mass in the explosive yields from WLW95/WLW93 and thus to calculate the stellar yields that correspond to this star. The yields are then multiplied by the number of stars given by $\Phi(m)$ for the initial (zero-age main-sequence) mass of the star.

Because the production of elements given by WLW93 and WLW95 is calculated only for stars with $Z = 0.02$, we have assumed that the relative yields for the other two abundances ($Z =$ 0.008 and 0.05) of the high mass-loss rate case are similar. Therefore we have calculated from the total ejected masses (the new elements and old ones) given by WLW93 and WLW95, the stellar yields, as new elements ejected by supernova as

$$p_i = m_{{\rm ej},i} - (m_* - m_{\rm rem}) * X_{i,0}, \quad (3)$$

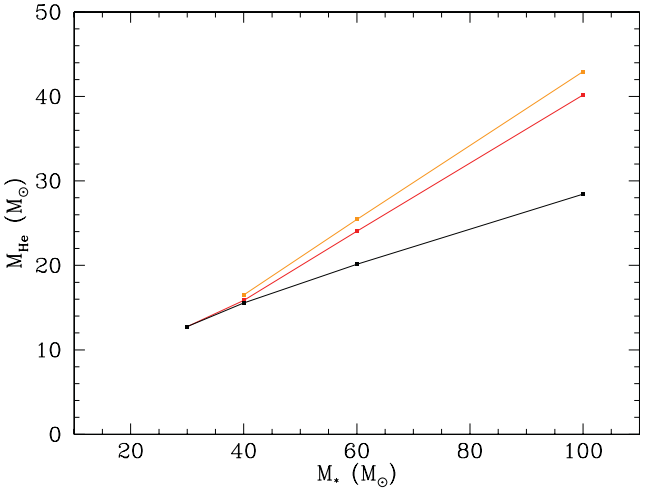

Figure 5. The relation between the He core mass $m_{\rm He}$, defined as the stellar mass when the H abundance is zero, and the initial stellar mass at the main sequence m_* for models with $m \geq 30\,{\rm M}_\odot$. Each line corresponds to a metallicity as labelled.

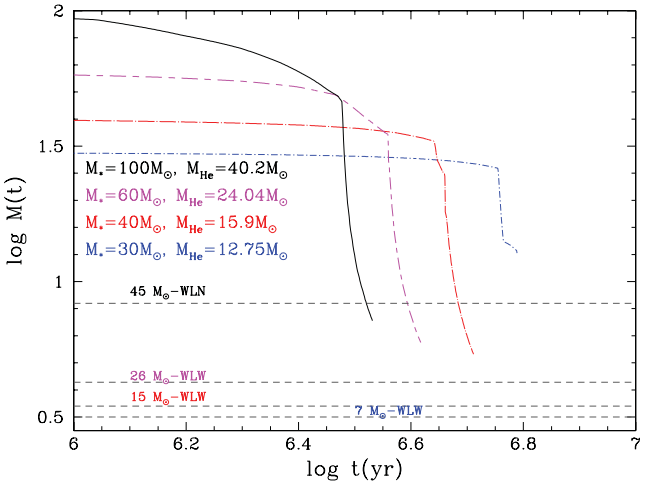

Figure 6. Evolution of the instantaneous mass in the higher mass stellar models. The horizontal lines give the WLW93/WLW95 final masses.

where Xi, 0 are the elemental abundances for each element i corresponding to $Z = 0.02$, and $m_{\rm rem}$ is the mass of the remnant. Then, we recalculated the ejected masses for each Z as

$$m_{{\rm ej},i} = p_i + (m_* - m_{\rm rem}) * X_{i,0} \quad (4)$$

for abundances $Z = 0.008$ and 0.05 using the same stellar yield p_i and substituting $X_{i,0}$ with the corresponding values.

The instantaneous mass fractions for He, C, N and O for the supernova ejecta are presented in Fig. 7. Since the ejected mass has no H for Type Ib/c supernova, we show all abundances as total mass fraction, as before. The dotted line indicates the reference value for $Z = 0.02$. Each colour indicates a different metallicity with the same coding than in previous Figs 3 and 4. For the three lowest Z only WW95 has been used, and so the evolution follows a continuous line. When $Z \geq 0.008$ we see the change from the ejecta of Type Ib supernova (originally WR stars), following WLW93/WLW95 stellar yields to the Type II supernova from WW95 ejecta as a sharp vertical line. The first ones produce less He and N and more C and O than the second ones. This behaviour is expected given that these stars ejected large quantities of He and N before to explode as supernova, during the stellar winds phase.

Table 5 gives the accumulated ejected masses by the Type Ib/c and Type II supernova explosions in each time step. For each IMF and metallicity given in columns 1 and 2, we show the time in column 3, the mass of the star which dies in this time in column 4, the mass of the He core in column 5, the remnant mass in column 6, the total ejected mass in column 7, and the ejected masses of H to O in columns 8–12.

The evolution of the accumulated or total abundances due to supernova ejections is illustrated in Fig. 8. A large increase in the O and C abundances is clearly seen at 4–6 Myr corresponding to the start of the supernova activity. After that there is a steady decrease reaching values around 2 times the initial values after almost 20 Myr. The He and N abundances, however, do not have an important contribution of Type Ib supernova and they maintain a constant high level after about 5 Myr due to the contribution of Type II supernova with lower mass progenitors.

4 THE TOTAL ABUNDANCES OF THE CLUSTER EJECTA

In this section we show the evolution of the stellar cluster abundances obtained by adding both contributions, winds and supernova explosions ejections.

In Fig. 9 we show the time evolution of the abundances. There we plot the contribution of winds by long dashed (blue) lines, the contribution coming from supernova with short dashed (green) lines and the total abundances with solid (red) lines. For He both contributions are more or less similar at the end of 20 Myr when $Z \geq 0.004$, so the abundance is a factor of 2 if wind ejections are considered compared to the usual calculations performed with supernova productions only. For the two lowest metallicities the ejected masses are a factor 2 or 3 smaller.

We see that stellar winds produce high abundances of C and O only for $Z \geq 0.004$. The level of $12 + \log({\rm O/H})$ doesn't increase for $Z \leq 0.004$, while for higher Z it reaches almost two orders of magnitude larger. N, however, shows higher abundances than expected for all metallicities, even for the two lowest ones. Although these results are not unexpected, since they are due to the mass-loss rate law that depends on Z, these abundances, not calculated before, may have important consequence over the interpretation of observations of H II regions.

When we analyse the same plots for supernovae, we see that now C and O show very high abundances, compared with the reference values, mainly for $Z \leq 0.004$, while He and N are roughly in the expected level for its metallicity. C and O are primary elements, produced directly from He created in the star. Therefore, their production is expected to be independent of the initial composition, whereas N is a secondary element produced in the CNO cycle at the expense of the initial C and O, so it is reasonable that it scales with the initial abundances.

A summary of these considerations is in Tables 6 and 7 where the accumulated masses ejected after 20 Myr by winds and by supernovae are given. In each one we give for each IMF and each metallicity the total mass ejected in $M_\odot$ and then the contributions of each element, H, He, C, N and O proceeding from stellar winds and from supernovae, respectively.

For C the contribution of winds is essential, the supernovae contribution being a factor of 10 smaller except for the lowest metallicities ($Z = 0.0001$, 0.0004 and 0.004) for which the ejected masses are insignificant. Also for N only a small contribution is due to

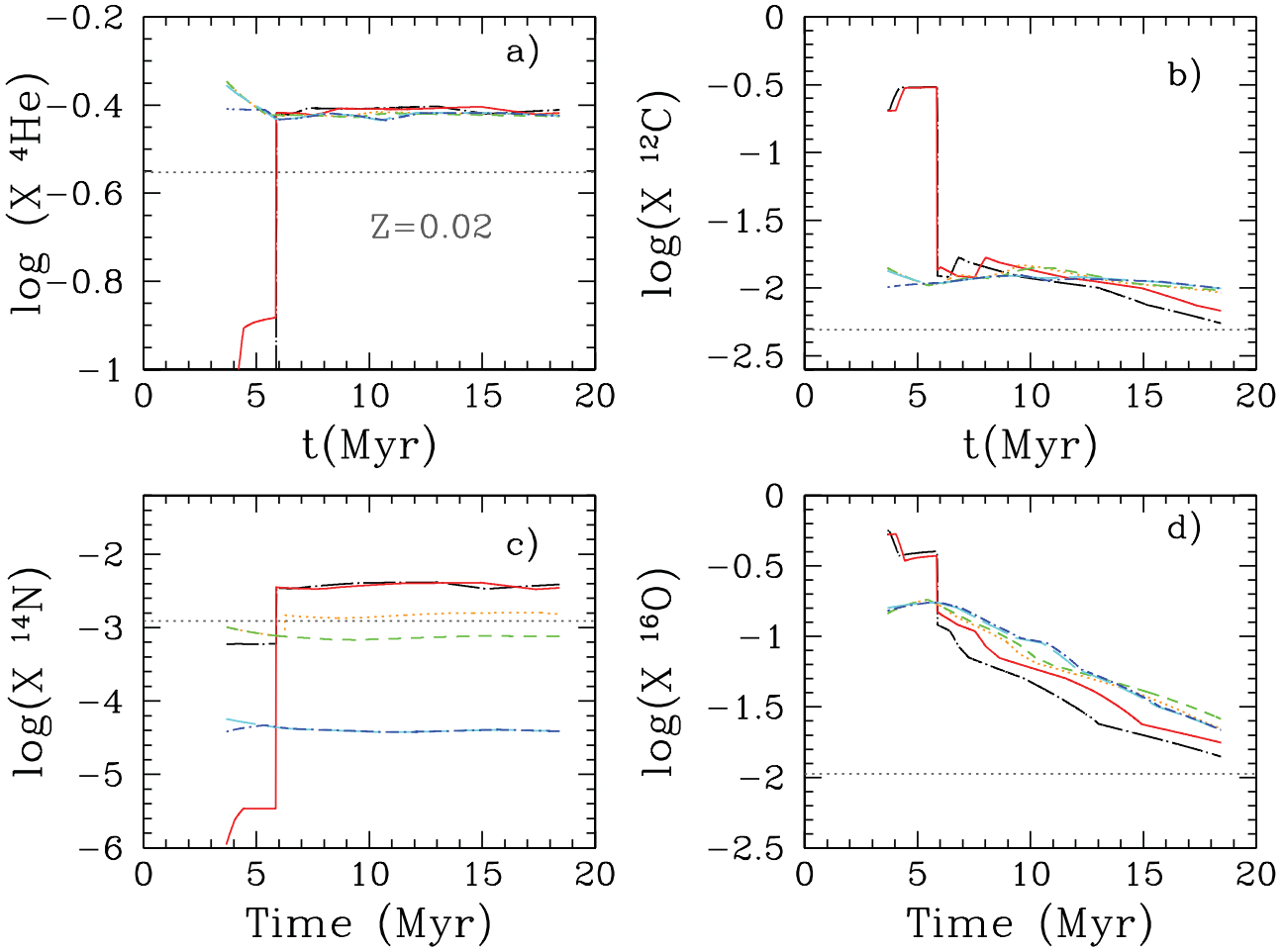

Figure 7. Evolution of the instantaneous values of He, C, N and O abundances in mass in the ejecta of a stellar cluster during the supernova phase. The line codification is the same as in Fig. 4.The dotted grey line marks the abundance $Z = 0.02$ in each panel.

Table 5. Accumulated masses ejected by stars dying as supernova explosions for a stellar cluster of 10^6 $M_\odot$ during the first 20 Myr for $Z = 0.02$ and a Salpeter IMF. The complete table with all times, metallicities and IMFs will be provided as Supporting Information with the online version of the article.

IMF	Z	Time (Myr)	m_* ($M_\odot$)	m_{He} ($M_\odot$)	m_{rem} ($M_\odot$)	m_{ej} ($M_\odot$)	H ($M_\odot$)	He ($M_\odot$)	C ($M_\odot$)	N ($M_\odot$)	O ($M_\odot$)
IMF	0.02	0.37700E+01	86.5627	34.7581	1.5500	0.2452E+01	0.0000E+00	0.1971E+00	0.4966E+00	0.3056E-05	0.1295E+01
IMF	0.02	0.37800E+01	85.5161	34.3357	1.5500	0.2698E+01	0.0000E+00	0.2169E+00	0.5465E+00	0.3403E-05	0.1425E+01
IMF	0.02	0.37900E+01	84.4982	33.9250	1.5500	0.2946E+01	0.0000E+00	0.2368E+00	0.5969E+00	0.3762E-05	0.1556E+01
IMF	0.02	0.38000E+01	83.5080	33.5255	1.5500	0.3196E+01	0.0000E+00	0.2570E+00	0.6476E+00	0.4130E-05	0.1689E+01
IMF	0.02	0.38100E+01	82.5443	33.1366	1.5500	0.3448E+01	0.0000E+00	0.2772E+00	0.6987E+00	0.4510E-05	0.1822E+01
IMF	0.02	0.38200E+01	81.6059	32.7580	1.5500	0.3702E+01	0.0000E+00	0.2977E+00	0.7502E+00	0.4900E-05	0.1956E+01
IMF	0.02	0.38300E+01	80.6921	32.3893	1.5500	0.3957E+01	0.0000E+00	0.3182E+00	0.8021E+00	0.5301E-05	0.2091E+01
IMF	0.02	0.38400E+01	79.8017	32.0300	1.5500	0.4214E+01	0.0000E+00	0.3389E+00	0.8543E+00	0.5713E-05	0.2227E+01

supernovae, at the end of the evolution, compared with the wind ejecta. For O the supernovae contribution is as important as the one from winds, particularly after 10 Myr of evolution. Therefore, the contributions of stellar winds to all abundances seem to be essential and must be taken into account in the evolution of stellar clusters and also in the galaxy evolution models in order to interpret adequately the data.

We show the final results for different IMFs in Fig. 10. There the fraction of mass ejected in the wind phase in panel (a) and the final abundances in panels (b) to (d) are represented as a function of Z for the six IMFs of this work. Results for MIL and FER show the smallest abundances of He, C and N, and the highest H values. The other IMFs show results very similar, lower than MIL and FER in H, higher for the other elements. In any case differences among IMFs results are relatively small.

5 CONCLUSIONS

We have computed the evolution of the total mass ejected and the elemental abundances of He, C, N and O for young stellar clusters of 10^6 $M_\odot$ for six IMFs and for six different initial metallicities.

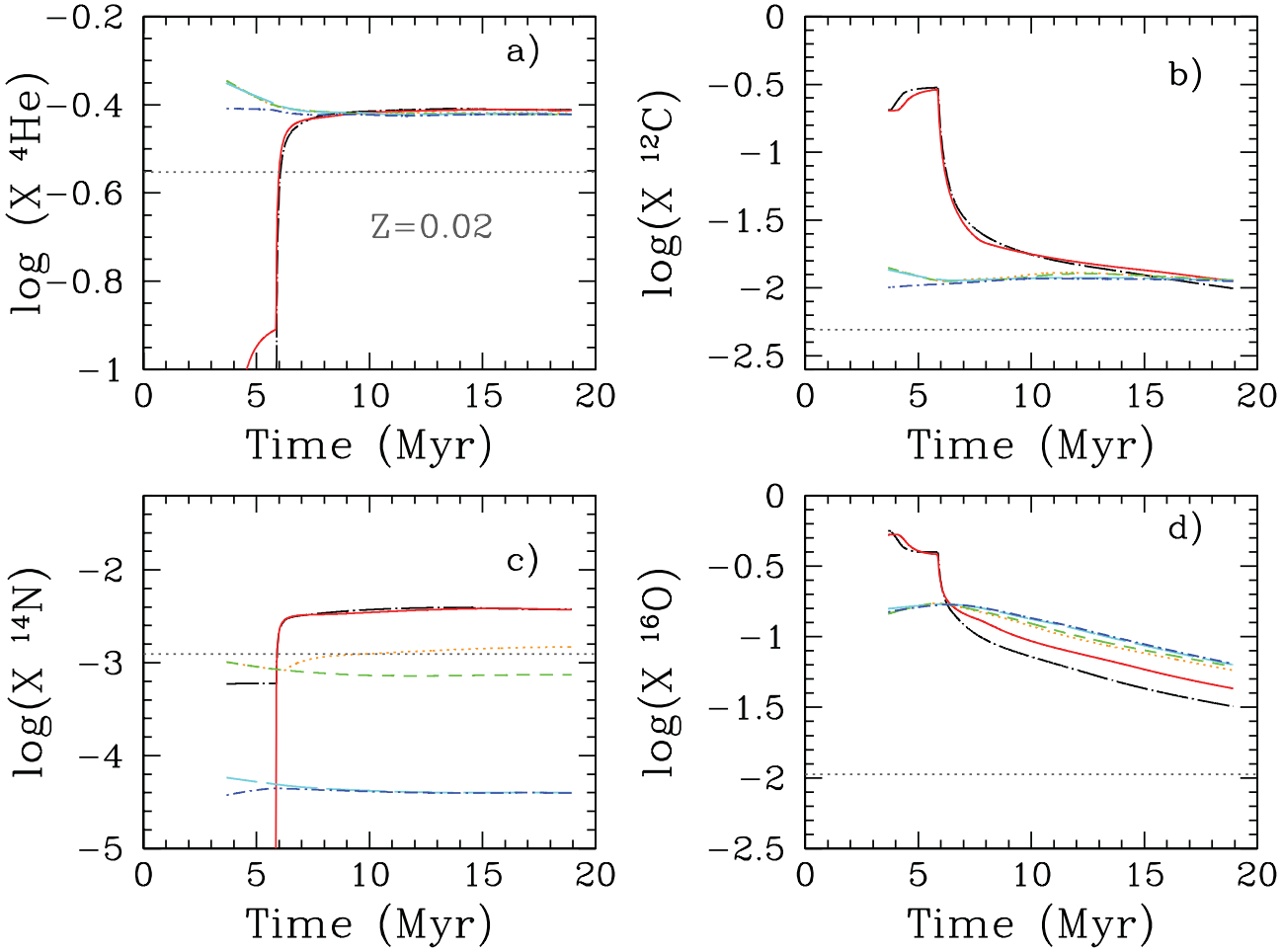

Figure 8. The evolution of the abundances in mass as $\log X$ of the accumulated ejected mass by a stellar cluster during the supernova phase for (a) He, (b) C, (c) N and (d) O for $Z = 0.02$ and a Salpeter IMF. The dotted grey line marks the reference abundance in each panel.

Both stellar wind and supernova contribution to the ejecta are included in the computations. The supernova contribution includes the classical gravitational collapse from WW95 for low-mass progenitors plus the yields calculated by WLW93 and WLW95 for stars more massive than 30 $M_\odot$ and with $Z \geq 0.008$ that reach the supernova stage after completely losing their H envelope.

The abundances of the ejecta obtained by adding both contributions show important differences in comparison with the standard method which uses only supernova yields without taking into account the stellar wind yields and/or the difference in the supernova yields resulting from the huge mass loss affecting the pre-supernova evolution.

In particular, we note the following.

(i) The composition of the ejected matter is determined mostly by supernova at low metallicities and by stellar winds at around solar metallicities.

(ii) The total mass ejected by stellar winds ranges from about 1 per cent of the initial cluster mass for the lowest metallicity model to about 6 per cent for the ∼solar abundance ones of the total mass of the cluster for a Salpeter IMF.

(iii) The total mass ejected by supernova is ∼5 per cent of the total mass of the cluster for all initial metallicities.

(iv) At high metallicities the proportion of the mass ejected by the winds phase is around 40–60 per cent of the total ejecta.

(v) There is a large increase in the abundance of He, C, O and N after 2.5 Myr with O and C abundances being the most extreme. The O abundance jumps almost two orders of magnitude between 2.5 and 4 Myr in our lowest metallicity model and about three times for the solar abundance model. Between 2 and 3 Myr, the C abundance increases between 10 and 30 times its initial value depending on the initial abundance.

(vi) He and N show more moderate jumps than C and O in their abundance between 2.5 and 4 Myr. He abundance increases almost three times for the solar value models and about two times for $Z = 0.0004$. On the other hand, N shows jumps of about five times for all abundances. For cluster ages $t < 10$ Myr, He and N enrichment is mainly due to the stellar winds.

These huge variations in the abundances of the ejecta of a stellar cluster can have a profound effect in the hydrodynamical evolution of the ISM. The high metallicity of the young cluster ejecta will lead to extremely short cooling times with important consequences for the subsequent feedback.

On the other hand, one should keep in mind the main shortcomings and uncertainties of our models.

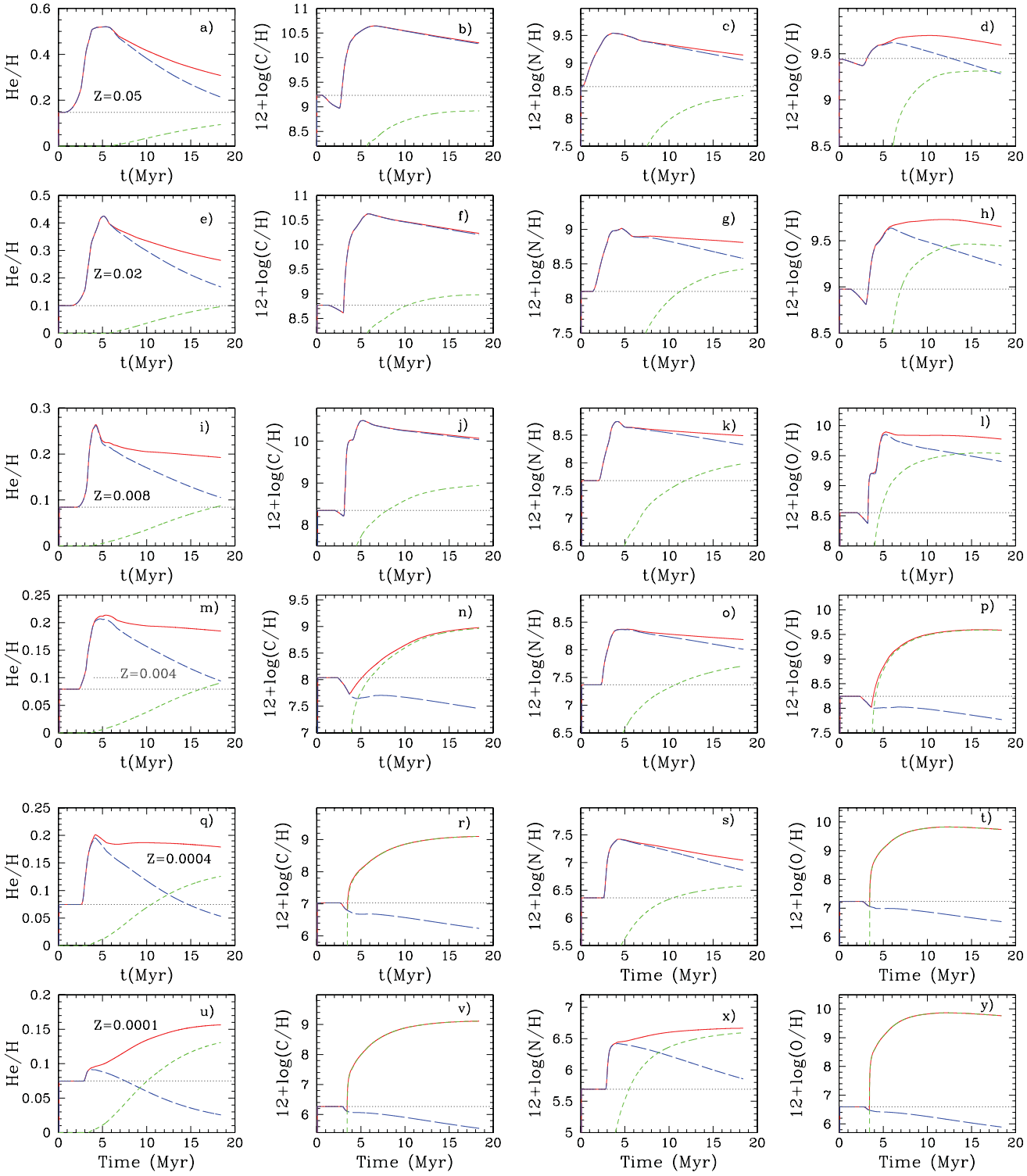

Figure 9. Evolution of the total abundances of the ejecta of a young stellar cluster with a Salpeter IMF due to stellar winds and supernova. Stellar wind contribution: blue long dashed lines; supernova contribution: short dashed green lines. Total: red solid line. The dotted grey line marks the solar abundance in each panel. The initial abundances are from top to bottom $Z = 0$, 05, 0.02, 0.008, 0.004, 0.0004 and 0.0001. The elemental abundances are from left to right for He/H, C/H, N/H and O/H.

Table 6. Total masses ejected by stellar winds for a cluster at the end of the wind phase for all abundances and IMFs.

IMF	Z	m_{ej} ($M_\odot$)	H ($M_\odot$)	He ($M_\odot$)	C ($M_\odot$)	N ($M_\odot$)	O ($M_\odot$)
SAL	0.0001	12 787	9363	3423	0	0	0
SAL	0.0004	18 080	10 881	7453	1	4	2
SAL	0.0040	41 407	24 726	18 598	17	71	47
SAL	0.0080	52 781	27 930	22 485	6933	160	2157
SAL	0.0200	62 677	24 161	34 006	9683	269	1392
SAL	0.0500	70 809	22 410	40 487	10 853	759	1446
MIL	0.0001	2862	2106	753	0	0	0
MIL	0.0004	4362	2751	1646	0	1	1
MIL	0.0040	13 721	8515	5656	7	21	18
MIL	0.0080	17 733	10 159	6807	1920	47	636
MIL	0.0200	21 829	9598	10 953	3253	85	461
MIL	0.0500	26 913	9890	13 988	4567	218	599
FER	0.0001	2190	1607	582	0	0	0
FER	0.0004	3200	1968	1268	0	1	0
FER	0.0040	8553	5211	3679	4	14	10
FER	0.0080	10 966	6058	4422	1316	31	422
FER	0.0200	13 278	5498	6918	2021	54	288
FER	0.0500	15 719	5413	8538	2556	146	337
MAR	0.0001	32 920	20 437	7472	0	1	1
MAR	0.0004	46 307	23 750	16 270	2	8	4
MAR	0.0040	98 511	53 958	40 587	37	155	102
MAR	0.0080	128 362	60 948	49 078	15 132	349	4709
MAR	0.0200	151 042	52724	74 216	21 128	587	3038
MAR	0.0500	169 237	48 903	88 359	23 681	1656	3156
CHA	0.0001	19 514	14 286	5227	0	1	1
CHA	0.0004	27 528	16 540	11 381	1	5	3
CHA	0.0040	62 281	37 132	28 066	25	107	70
CHA	0.0080	79 380	41 850	33 976	10 484	242	3254
CHA	0.0200	94 122	36 074	51 222	14 535	406	2093
CHA	0.0500	105 977	33 317	60 835	16 132	1148	2155
KRO	0.0001	18 392	13 464	4926	0	0	1
KRO	0.0004	25 946	15 589	10 727	1	5	3
KRO	0.0040	58 700	34 998	26 452	24	101	66
KRO	0.0080	74 816	39 444	32 023	9881	228	3067
KRO	0.0200	88 711	34 000	48 277	13 699	383	1973
KRO	0.0500	99 885	31402	57 338	15 205	1082	2031
STB	0.0001	25 645	18 777	6865	0	1	1
STB	0.0004	36 260	21 821	14 947	1	7	4
STB	0.0040	83 041	49 587	37 297	34	142	94
STB	0.0080	105 851	56 013	45 094	13 903	321	4326
STB	0.0200	125 698	48 455	68 198	19 418	540	2792
STB	0.0500	142 007	44 943	81 196	21 766	1521	2900

Table 7. Total masses ejected by supernova for a cluster at the end of the supernova phase for each computed metallicity.

IMF	Z	M_{ej} ($M_\odot$)	H ($M_\odot$)	He ($M_\odot$)	C ($M_\odot$)	N ($M_\odot$)	O ($M_\odot$)
SAL	0.0001	46 230	24 090	17 510	521	2	3089
SAL	0.0004	46 520	24 230	17 670	529	2	3058
SAL	0.0040	47 510	24 800	17 980	549	35	3018
SAL	0.0080	49 020	25 610	18 690	563	72	2934
SAL	0.0200	50 460	26 510	19 530	581	189	2246
SAL	0.0500	46 240	25 050	17 870	468	173	1522
MIL	0.0001	36 540	19 470	13 850	410	1	2093
MIL	0.0004	36 860	19 650	13 990	416	1	2076
MIL	0.0040	38 750	20 630	14 650	443	29	2164
MIL	0.0080	40 880	21 760	15 570	463	62	2138
MIL	0.0200	45 560	24 180	17 660	492	171	1821
MIL	0.0500	41 880	22 880	16 200	390	157	1236
FER	0.0001	16 310	8635	6179	183	1	978
FER	0.0004	16 440	8706	6238	186	1	969
FER	0.0040	17 150	9078	6484	196	13	994
FER	0.0080	17 990	9531	6855	205	27	977
FER	0.0200	19 690	10 420	7626	216	74	808
FER	0.0500	18 080	9860	6991	172	68	548
MAR	0.0001	100 900	52 600	38 240	1138	4	6752
MAR	0.0004	101 600	52 900	38 590	1156	4	6687
MAR	0.0040	103 700	54 120	39 270	1198	77	6596
MAR	0.0080	107 000	55 890	40 800	1230	158	6410
MAR	0.0200	110 100	57 830	42 610	1269	412	4903
MAR	0.0500	100 900	54 660	38 990	1022	377	3323
CHA	0.0001	66 310	34 510	25 120	748	3	4476
CHA	0.0004	66 720	34 700	25 340	759	3	4430
CHA	0.0040	68 000	35 440	25 750	786	51	4357
CHA	0.0080	70 060	36 550	26 710	806	103	4231
CHA	0.0200	71 700	37 640	27 750	830	269	3215
CHA	0.0500	65 690	35 570	25 380	670	246	2179
KRO	0.0001	62 490	32 520	23 670	705	2	4218
KRO	0.0004	62 890	32 700	23 880	716	3	4176
KRO	0.0040	64 090	33 400	24 270	741	48	4107
KRO	0.0080	66 040	34 450	25 180	760	97	3988
KRO	0.0200	67 580	35 470	26 150	782	253	3031
KRO	0.0500	61 920	33 520	23 920	631	232	2054
STB	0.0001	92 710	48 320	35 120	1046	4	6195
STB	0.0004	93 300	48 600	35 430	1061	4	6133
STB	0.0040	95 280	49 730	36 070	1100	71	6052
STB	0.0080	98 310	51 360	37 480	1130	145	5883
STB	0.0200	101 200	53 160	39 170	1165	379	4504
STB	0.0500	92 740	50 240	35 840	939	347	3053

Because present stellar evolutionary models with mass loss do not include the supernova phase and supernova models do not cover a range in initial abundances, our adopted values for the supernova yields of the most massive stars are only approximate.

Binary evolution is not considered. It is known that in young massive clusters perhaps all massive stars are in binary or multiple systems, but it is not clear how the presence of a companion would affect the properties of wind of a massive star.

The effect of stellar rotation is not included in the stellar evolution models we have used. Again, as in the case of binaries, it is not clear at this stage how rotation would affect the wind of a massive star.

In spite of these warnings, our models should be useful for the interpretation of the evolution of the ISM in star-forming galaxies. The resulting tables are available as Supporting Information with the online version of the article.

ACKNOWLEDGMENTS

This work has been partially supported by DGICYT grant AYA2010–21887–C04–02. Also, by the Comunidad de Madrid under grant CAM S2009/ESP-1496 (AstroMadrid) and by the Spanish MICINN under the Consolider-Ingenio 2010 Program grant CSD2006-00070: First Science with the GTC.[3] RT is grateful to the Mexican Research Council (CONACYT) for supporting this research under grants CB-2006-49847, CB-2007-01-84746 and CB-2008-103365-F. We would like to thank Elena Terlevich and the referee Rafael Hirschi for many suggestions that greatly improved this paper. Dedicated to the memory of M.F.B.

[3] http://www.iac.es/consolider-ingenio-gtc

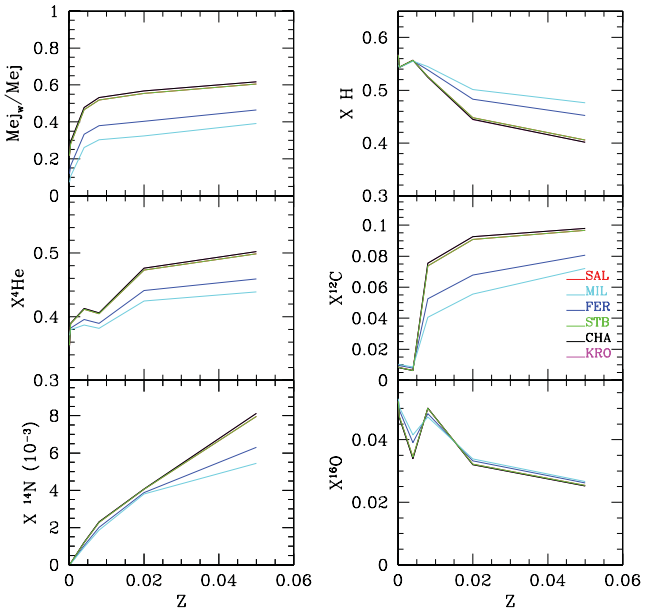

Figure 10. The dependence of the final ejected masses with the metallicity for different IMFs as labelled.

REFERENCES

Asplund M., Grevesse N., Sauval A. J., Scott P., 2009, ARA&A, 47, 481
Bressan A., Fagotto F., Bertelli G., Chiosi C., 1993, A&AS, 100, 647
Cerviño M., Luridiana V., 2004, A&A, 413, 145
Cerviño M., Luridiana V., 2006, A&A, 451, 475
Chabrier G., 2003, ApJ, 586, L133
Chieffi A., Limongi M., 2004, ApJ, 608, 405
Dray L. M., Tout C. A., 2003, MNRAS, 341, 299
Dray L. M., Tout C. A., Karakas A. I., Lattanzio J. C., 2003, MNRAS, 338, 973
Fagotto F., Bressan A., Bertelli G., Chiosi C., 1994a, A&AS, 104, 365
Fagotto F., Bressan A., Bertelli G., Chiosi C., 1994b, A&AS, 105, 29
Ferrini F., Penco U., Palla F., 1990, A&A, 231, 391
Fröhlich C. et al., 2006, ApJ, 637, 415
Heger A., Woosley S. E., 2010, ApJ, 724, 341
Hirschi R., 2007, A&A, 461, 571
Hirschi R., Meynet G., Maeder A., 2005, Nucl. Phys. A, 758, 234
Kobayashi C., Umeda H., Nomoto K., Tominaga N., Ohkubo T., 2006, ApJ, 653, 1145
Kobulnicky H. A., Skillman E. D., 1998, ApJ, 497, 601
Kobulnicky H. A., Skillman E. D., Roy J.-R., Walsh J. R., Rosa M. R., 1997, ApJ, 477, 679
Kroupa P., 2001, MNRAS, 322, 231
Leitherer C. et al., 1999, ApJS, 123, 3 (STB99)
Limongi M., Chieffi A., 2003, ApJ, 592, 404
López-Sánchez Á. R., Esteban C., 2010, A&A, 517, A85
Maeder A., 1992, A&A, 264, 105
Meynet G., Maeder A., 2002, A&A, 390, 561
Miller G. E., Scalo J. M., 1979, ApJS, 41, 513
Portinari L., Chiosi C., Bressan A., 1998, A&A, 334, 505 (PCB98)
Rauscher T., Heger A., Hoffman R. D., Woosley S. E., 2002, ApJ, 576, 323
Raymond J. C., Cox D. P., Smith B. W., 1976, ApJ, 204, 290
Salpeter E. E., 1955, ApJ, 121, 161
Silich S. A., Tenorio-Tagle G., Terlevich R., Terlevich E., Netzer H., 2001, MNRAS, 324, 191
Tenorio-Tagle G., 1996, AJ, 111, 1641
Umeda H., Nomoto K., 2002, ApJ, 565, 385
van Zee L., Haynes M. P., 2006, ApJ, 636, 214
Woosley S. E., Weaver T. A., 1995, ApJS, 101, 181 (WW95)
Woosley S. E., Langer N., Weaver T. A., 1993, ApJ, 411, 823 (WLW93)
Woosley S. E., Langer N., Weaver T. A., 1995, ApJ, 448, 315 (WLW95)

SUPPORTING INFORMATION

Additional Supporting Information may be found in the online version of this article:

Table 2. Surface abundances of the stellar models.
Table 3. Accumulated masses ejected by a stellar cluster during its wind phase.
Table 5. Accumulated masses ejected by stars dying as supernova explosions.

Please note: Wiley-Blackwell are not responsible for the content or functionality of any supporting materials supplied by the authors. Any queries (other than missing material) should be directed to the corresponding author for the article.

This paper has been typeset from a TEX/LATEX file prepared by the author.